Journal of Materials Science Research; Vol. 2, No. 4; 2013
ISSN 1927-0585 E-ISSN 1927-0593
Published by Canadian Center of Science and Education

Vibro-Acoustic Characterization and Optimization of Periodic Cellular Material Structures (PCMS) for NVH Applications

Mohammad Al-Zubi[1], Emmanuel Ayorinde[2], Gary Witus[2], Mehmet Dundar[2], Manjinder Warriach[2] & Yellapu Murty[3]

[1] Mechanical Engineering Department, Tafila Technical University, Jordan

[2] Department of Mechanical Engineering, Wayne State University, Detroit, USA

[3] MC Technologies, 1163 River Chase Ridge, Charlottesville, VA 22901, USA

Correspondence: Emmanuel Ayorinde, Department of Mechanical Engineering, Wayne State University, Detroit, MI 48202, USA. Tel: 1-313-577-5488. E-mail: aa0983@wayne.edu

Received: May 28, 2013 Accepted: June 24, 2013 Online Published: September 5, 2013

doi:10.5539/jmsr.v2n4p64 URL: http://dx.doi.org/10.5539/jmsr.v2n4p64

Abstract

NVH (Noise, vibration, and harshness) performance has been identified as having a significant influence in the purchase considerations of most automobile purchasers. Periodic cellular material structures (PCMS) are recently introduced multi-functional structures, commonly in sandwich form, that facilitate a wide variety of engineering purposes. Although literature concerning many PCMS properties is abundant, information about their vibration and acoustic responses is scanty, to the best knowledge of the present authors. This article documents a basic investigation of the vibration and acoustic behaviors of some PCMS through practical, analytical and numerical approaches, in order to evaluate the possibilities for minimizing, the transmission of noise and vibration. Some of these materials were made and investigated over frequency ranges which include several commonly-encountered vibration and acoustic frequencies of automotive and some other structures. Observations from this work are therefore expected to contribute towards design inputs to obtain better performances. A novel investigation of the effects upon vibration response of even slight inaccuracies of cutting out samples from larger blanks of such materials has also been made.

Keywords: periodic cellular material, vibro-acoustic, NVH, frequency response functions, acoustic absorption

1. Introduction

NVH issues are critical to land, sea and air transportation vehicles for both civilian and military applications. The operating environment, materials of construction used to design the vehicle body as well as the machinery providing the power/propulsion to the vehicle govern the NVH performance, and ultimately affect the vehicle performance, and the safety, comfort, and wellbeing of the passengers in the vehicle. Often times the NVH factors control the speed limits and operational limitations of a vehicle. Noise is normally taken to mean unwanted sound, and vibration the periodic to-and-fro mechanical motion. Harshness is variously denoted in the automotive industry, but is generally described as an aggressive feel, or a very high resistance to a solitary input, or absence of perceptible displacement in response to a single input. This behavior can also be associated with a sharp thumping noise. It is often experienced in the low frequency range of about 15 Hz to 100 Hz.

Fabric like materials, elastomeric materials (such as rubber), metallic and polymeric foam materials, honeycomb structures, and a variety of sandwich constructions have been evaluated in order to control noise and vibration behavior inside the vehicles (Zent & Long, 2007; Al-Zubi, 2012). While fabric-like materials are highly efficient as acoustic absorbers, they are not effective in reducing vibration. Traditional honeycomb materials, due to their rigid architecture, seriously limit design options. Polymeric and elastomeric designs were used to mitigate shock (sharp impacts), and to a lesser extent to contain vibration effects.

Vibro-acoustic sandwich designs facilitating complex shapes such as doors, interior panels, exterior shrouding around rotating machinery, etc., can open up promising opportunities for better vehicle designs. One such higher archival structural material family, the Periodic Cellular Material Structures (PCMS), presently undergoing intense development in industry under the trade name MicroTruss® sandwich panels, offer a great potential.

These PCMS are structurally strong, offering potential multifunctional attributes. They are made with open- and closed-cell topologies, and exhibit excellent weight/bend stiffness ratio.

Periodic cellular materials have been applied in thermal isolation, cross-flow heat exchangers, light-weight load support, channels for routing electrical wiring, current collectors for novel battery systems, and catalyst support for chemical reactions (Wadley, 2002; Sypeck & Wadley, 2002; Wadley, Fleck, & Evans, 2003; Tian et al., 2004; Queheillalt et al., 2008; Wei et al., 2008). More applications are still coming on stream. Although many aspects of the response of periodic cellular material structures have been examined in the foregoing and other references, the vibration and acoustics aspects seem to not have been looked at for PCMS beyond the metal honeycomb structure (Chevillotte, Perrot, & Pennelton, 2010). Even there, the only ways advocated to increase the acoustic performance of the metal foam are to use open-cell foam or perforated closed cell foams with continuous flow paths for sound. Both approaches are high in manufacturing costs. Non-foam type PCMS of different constructions are now being used. The question of how these PCMS types perform vibro-acoustically, and how to possibly improve such performances if found to be inadequate, appear to not have been addressed. The overall goal of the research mentioned in this work is to advance the comprehension of the vibro-acoustic characteristics of MicroTruss® sandwich periodic cellular material structures in order to establish the technology and design methodologies through the use of constitutive modeling and experimental-cum-numerical verification. It also aims to develop the deliberate design of PCMS in order to obtain efficient acoustic absorption and vibration mitigation at targeted frequencies and frequency bands.

2. Vibro-Acoustic Treatments for PCMS Components

PCMS are in general composed of variously-contrived assemblages of elements such as plates, bars, rods, balls, meshes of different degrees of fineness, made of a number of several materials, as appropriate to the intended use. In the consideration of effective treatments for PCMS, it is therefore proper to examine viable vibro-acoustic treatments of such constituent components. For passive vibration control, Birman (2005) utilized pre-stressed shape memory alloy wires embedded in such plates to provide an elastic foundation support and hysteretic energy dissipation by the super elastic wires as they vibrated with the plate. Xu et al. (2009) employed topology optimization to control both vibration eigen-frequencies and radiated sound power by finding the best distribution of volumetric density over the finely discretized domain. Fang, Li and Fu (2012) utilized constrained layer damping by adhering visco-elastic material to the surfaces of beams and plates to passively damp out vibrations. Active control of vibration and damping of plates and other structures have also been explored and utilized. For example, Karganovin, Najavizadeh, and Viliani (2007) used piezoelectric actuators and sensors to actively control the vibration of a functionally graded plate using a steady electric current. However, passive control is normally so much simpler and cheaper if feasible.

Some measures have also been used to mitigate sound in various structural components. De Bedout et al. (1997) utilized a self-tuning Helmholtz resonator to achieve up to 30 dB of noise reduction. Pfretzchner and Rodriguez (1999) studied the acoustics of rubber crumbs as a function of particle size, layer thickness and spatial distribution, and suggested that similar constructions of other materials would achieve different sound absorption capabilities. Hong et al. (2007) continued this approach by adding a second layer, respectively made of foam and perforated panel to reduce the sound, while Yu and Cheng (2009) used an array of a geometrically more complex (T-shape), pneumatically controlled acoustic absorbers.

3. Theory

The wave impedance and propagation constant can be calculated by considering the equation of motion of an infinitesimal layer, thickness dx, of the vibrating medium, as shown in

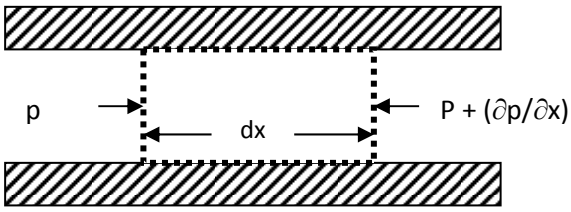

Figure 1. Acoustic element

The equation of motion, ignoring damping effects for simplicity, may, from developments in various texts, be rendered as

$$-\frac{\partial p}{\partial x} = \rho_0 \frac{\partial v}{\partial t} \tag{1}$$

where p is pressure, ρ_0 is the air density, x is coordinate and v is velocity. The continuity equation is

$$-\frac{\partial v}{\partial x} = \frac{1}{\rho_0}\frac{\partial \rho}{\partial t} = \frac{1}{K_0}\frac{\partial p}{\partial t} \tag{2}$$

where $K_0 = \frac{dp}{d\rho / \rho_0}$

Following standard developments, the acoustic absorption coefficient for normal incidence may finally be obtained as

$$a_0 = \frac{4\,\mathrm{Re}(z / \rho_0 c_0)}{(\mathrm{Re}(z / \rho_0 c_0) + 1)^2 + (\mathrm{Im}(z / \rho_0 c_0))^2} \tag{3}$$

Dynamic equilibrium equations of the completely free circular plate leading to the vibration equations can be formulated with Bessel functions. Using the Bessel function of the first kind, J, and the modified Bessel function of the first kind, I, the characteristic equation for a free circular plate, radius a, in transverse vibration may be written as,

For n = 0,

$$\gamma a\,\{J_0(\gamma a)I_1(\gamma a) + J_1(\gamma a)I_0(\gamma a)\} - 2(1-\nu)J_1(\gamma a)I_1(\gamma a) = 0 \tag{4a}$$

For n > 0,

$$\{(\gamma a)^4 + n^2(n^2-1)(1-\nu)^2\}\{J_{n-1}(\gamma a)I_{n+1}(\gamma a) + J_{n+1}(\gamma a)I_{n-1}(\gamma a)\} - 2n(1-\nu)(\gamma a)^2\{(n-1)\,J_{n-1}(\gamma a)I_{n-1}(\gamma a) + (n+1)J_{n+1}(\gamma a)I_{n+1}(\gamma a)\} = 0 \tag{4b}$$

The roots of the equations are the infinite number of eigenvalues, γ_{mn}, with number of nodal diameters, m, and number of nodal circles, n, as subscripts. The mode-shapes are supplied by the eigenvectors, W_{mn}, which are given by

$$W_{mn}(r,\theta) = [J_n(\gamma_{mn} r) - \sigma_{mn} I_n(\gamma_{mn} r)]\cos n\theta \tag{5a}$$

where

$$\sigma_{mn} = \frac{n(n-1)(1-\nu)J_n(\gamma_{mn}a) - (\gamma_{mn}a)(2n+1+\nu)J_{n+1}(\gamma_{mn}a) + (\gamma_{mn}a)^2 J_{n+2}(\gamma_{mn}a)}{n(n-1)(1-\nu)I_n(\gamma_{mn}a) + (\gamma_{mn}a)(2n+1+\nu)I_{n+1}(\gamma_{mn}a) + (\gamma_{mn}a)^2 I_{n+2}(\gamma_{mn}a)} \tag{5b}$$

It was found in our work that the use of Rayleigh's approximate energy method for natural frequency under-predicted the natural frequency by only 6% relative to the Bessel function solution, thus making it acceptable for engineering purposes.

4. Materials

The three PCMS materials investigated were the aluminum pyramidal core MicroTruss® PCMS, aluminum prismatic (triangular-channel) MicroTruss® and stainless steel triangular honeycomb PCMS. The material of the aluminum samples is aluminum 6061 T6, and the steel is stainless steel 304. The pictures and sketches are shown in Figure 2. These materials were chosen as representatives of PCMS materials class, of which there has not been any systematic vibro-acoustic testing reported in the literature. The major attraction of these materials is their high stiffness-to-weight and strength-to-weight ratios, coupled with high multi-functionality as earlier detailed in the introduction.

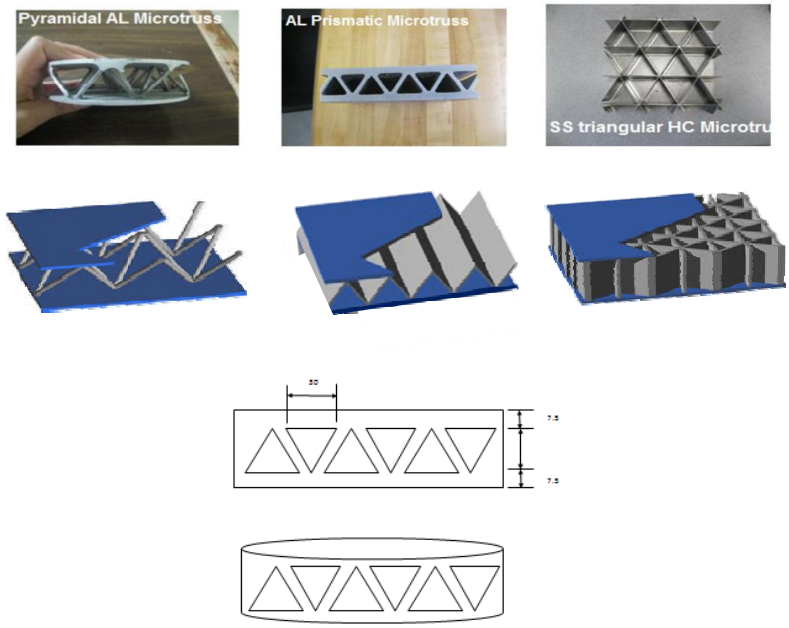

Figure 2. Images of test materials (pictures) and sketches of prismatic aluminum PCMS sample

5. Experimental Work

The "PULSE" 14.0 (and later the 16.1 with the software Pulse Reflex 16.1) vibro-acoustic instrumentation and software platform was utilized in our experiments, along with the impedance tube, impact hammer and accelerometers, all from Bruel & Kjaer, Inc., as well as some PCB impact hammers, were used in the experiments. The tube utilized was the B&K Two-Microphone Impedance Measurement Tube Type 4206, fitted with two specially designed ¼-inch microphones. Specimens of diameters 100 mm and 29 mm were cut from each material for acoustic absorption tests, and the larger samples were also subjected to impact response vibration tests. Results were obtained from experimental, analytical and numerical approaches. Figures 3 and 4 are sketch illustrations of essential parts of the experimental setups.

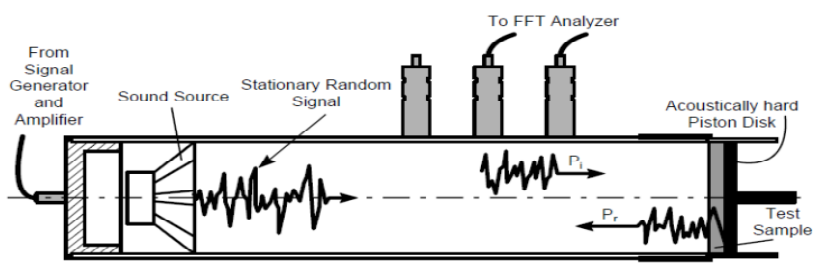

Figure 3. Sketch of the 2-microphone impedance method

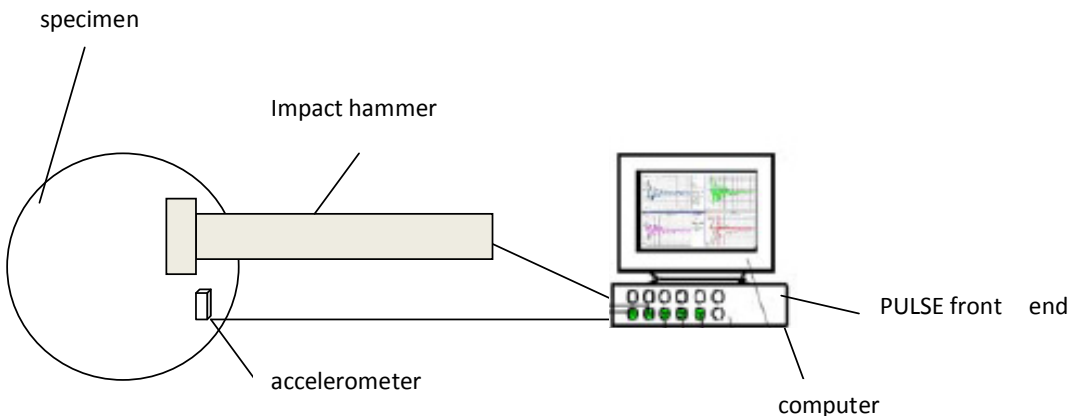

Figure 4. Sketch of the impact FRF test

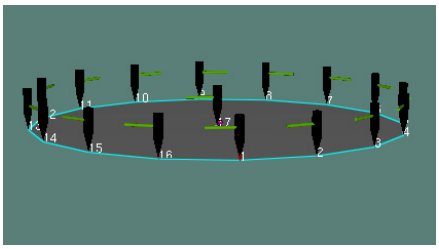

Figure 5. Geometry used in Pulse modal software and the Hammer hit points-accelerometer at point 1

For the frequency response (FRF) test, as shown in Figure 4, the hammer hit is near the response sensor attachment. In the full modal test, we used 17 roving hammer points. The 29 mm and 100 mm diameter tubes which accommodate the small and larger specimens respectively were used for acoustic absorption tests in the 50 Hz to 1600 Hz range, and the 500 Hz to 6400 Hz ranges respectively. The high-pass filter was utilized for the small tube, and the linear for the large tube. The accelerometers used were sensitive to about 50 kHz. The PULSE system had outstanding frequency features such as the combination of measured data in overlapping frequency ranges, concurrent graphical display of multiple sets of measured data, averaging of up to ten sets of measured data, as well as data file management on hard or floppy disc drive, and also hard copy facilities in tabular and graphical forms.

6. Numerical Methods

The numerical methods employed are the Nastran and Abaqus Finite Element methods and the Matlab numerical solutions package. Vibration eigen-solutions were obtained via the Nastran procedure to calculate the eigen-values (natural frequencies) and eigen-vectors (mode shapes) for circular plates, using the pre- and post-processor Hypermesh (version 10 from Altair Engineering Inc.) for the selected frequency range 0 to 10,000 Hz. A total of 9432 pshell elements were utilized with a triangular mesh of density 250 using the sol 103 (for normal modes) solution procedure. For the Abaqus procedure, all samples were also meshed by using the Hypermesh as a preprocessor, and then Abaqus/Standard 3D was used as a solver to calculate the first three natural frequencies and the mode shapes of the samples. The Lanczos Eigen-solver Method was selected in Abaqus/Standard 3D to determine the first three fundamental frequencies and mode shapes because this method is a powerful tool for extraction of the extreme eigen-values and the corresponding eigen-vectors of a sparse symmetric generalized eigen-problem. All samples were taken to be solid and the C3D4 (tetra4) element type was used. For Matlab solutions, some reference code (Yang, 2005) was utilized in writing a Matlab computer program to calculate the natural frequencies and animate their mode shapes.

7. Results and Discussion

7.1 Periodic Geometry Effects

The periodic structure of the PCMS materials presents a great opportunity for their use as efficient acoustic absorbers. Among other things, a confined space with a small point- or slit-opening will serve as a Helmholtz

resonator, which highly absorbs sound at different frequencies, depending on geometries of cavity and "neck" (connecting orifice). Firstly the optimal design of such parameters could be explored by parametric variations. Secondly, the "open" or hollow construction of PCMS furthermore facilitates the insertion of other materials (such as fabrics, foams, etc.) with high acoustic absorption in order to boost the absorption of the whole assembly. Systematic investigation of the best combinations of such materials and their locations for acoustic efficiency is also enabled by such an approach. Thirdly, with respect to vibration, it is well known that the square root of the ratio of effective stiffness to effective mass determines the natural frequency in a structural vibration mode. The design of PCMS can also utilize this fact in the positioning of some natural frequencies. This would normally be a trade-off since PCMS are multi-functional structures with competing demands upon them. Fourthly, the tailoring of various combinations of methods such as those earlier reviewed, for the typical sub-components of PCMS (Birman, 2005; Xu et al., 2009; Fang, Li, & Fu, 2012; Karganovin, Najafizadeh, & Vilani, 2007; de Bedout et al., 1997; Pfretzschner & Rodriguez, 1999; Hong et al., 2007; Yu & Cheng, 2009) could be explored to best contain unwanted sound and vibration in the enhanced design of these structures. A fifth and quite important consideration is the issue of meta-material behavior in both the acoustic and vibration domains. Meta-materials are periodic-arrangement materials whose structure confers on them unusual properties not normally observed in nature. The manifestation in the acoustic area is that at certain frequency bands dependent upon the structural construction the transmission of sound is severely or totally impaired. Vibration meta-materials similarly manifest severe vibration "transmission dips" or losses. The science and applications of meta-materials are still being developed. The vibro-acoustic goals of meta-material deployment are to achieve complete or almost complete acoustic and vibration absorption just by structural design. This is a tremendous advantage that promises many useful outcomes. The majority of current meta-material applications are in the magnetic and electrical fields, and involve micro- and nano-sized components. However it has been shown (Huang & Sun, 2010; Islam & Newaz, 2012; Ayorinde et al., 2012) that much larger structures are feasible as acoustic and vibration meta-materials. PCMS materials already satisfy the major requirement of periodicity or quasi-periodicity for the manifestation of meta-material behavior. However, on account of analytical and computational complexity, only relatively simple structures have so far been examined. From our preliminary work, in Figure 7(d) the severe dips/annihilations in vibration are observable for some frequency bands. As time progresses, deeper investigations would reveal how PCMS can be structurally tailored to show such vibration and acoustic meta-material gating effects at desired frequency bands.

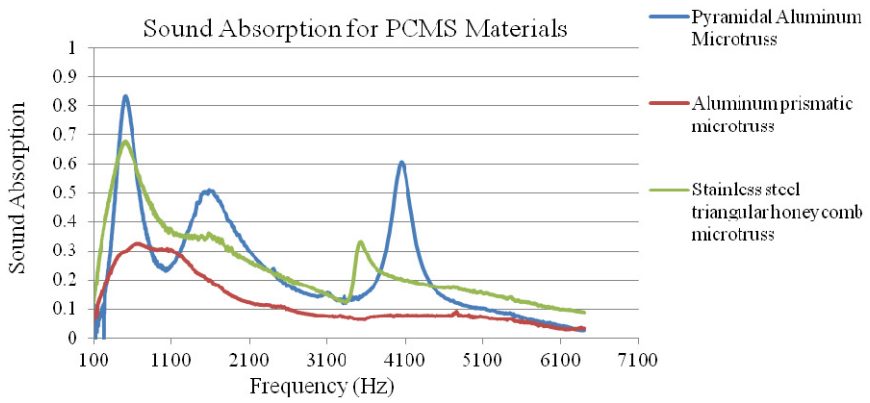

Figure 6. Sound absorption of some PCMS materials

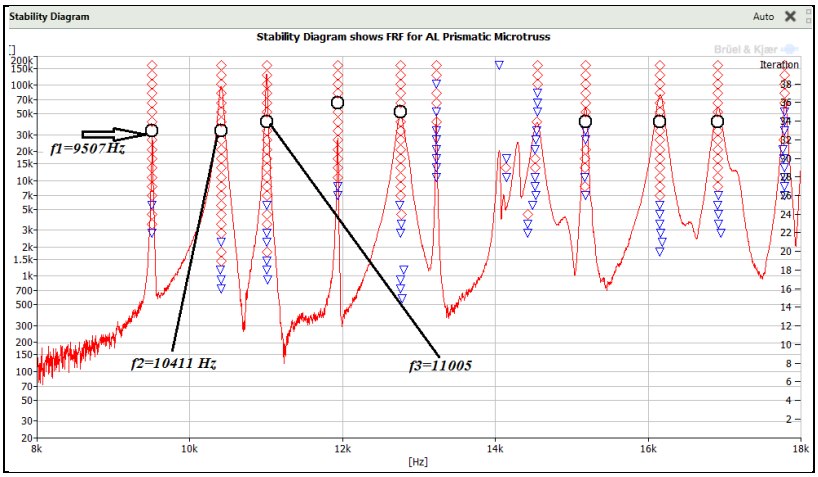

Figure 7. (a) Vibration spectrum of aluminum prismaticMicroTruss® PCMS material

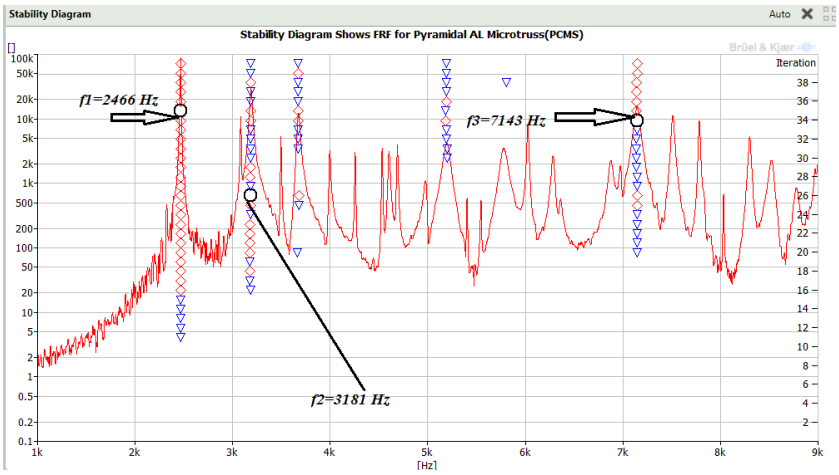

Figure 7. (b) Vibration spectrum of aluminum pyramidal MicroTruss®TM PCMS material

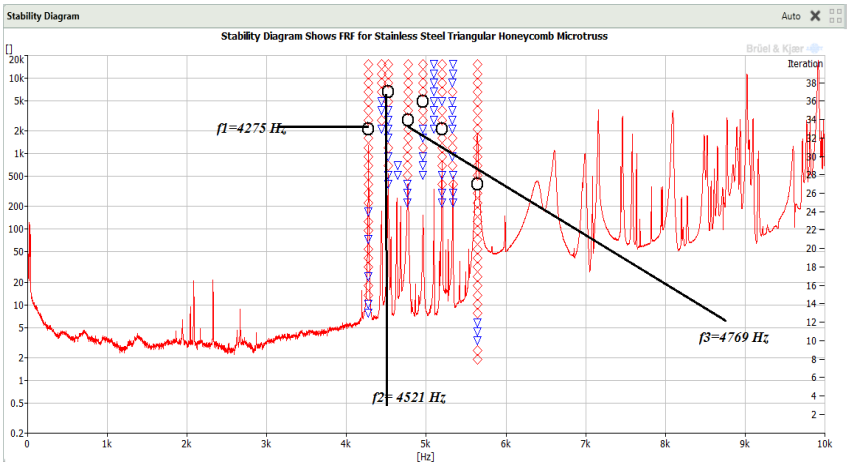

Figure 7. (c) Vibration spectrum of stainless steel triangular honeycomb PCMS

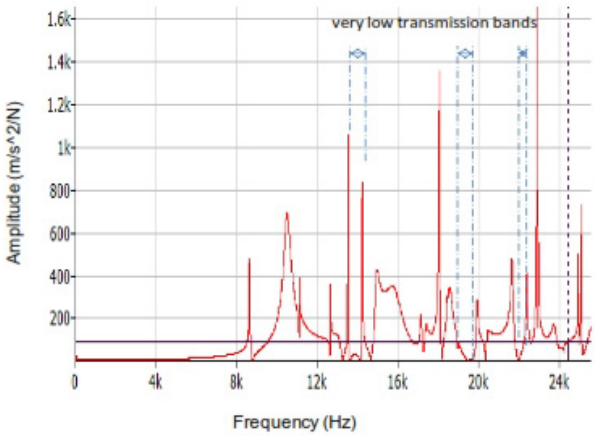

Figure 7. (d) Vibration spectrum of a typical aluminum prismatic (triangular-channel) MicroTruss® PCMS showing transmission dips

7.2 Acoustic Absorption

Acoustic absorption is essentially the dissipation of acoustic energy as heat, which process may also be described as the conversion of sound energy to thermal energy. The two ways in which this occurs are from visco-thermal boundary layers as air crosses orifices, and secondly the alternate expansion and contraction of the air column as it vibrates. In a structure set into motion, the relative proportion of the effective stiffness to the effective mass is the primary determinant of the characteristics (resonance frequencies and mode shapes) of the resonance phenomenon, and in an enclosure, the coupling between the walls and the enclosed air contributes to this determination for vibration and acoustics. There are many such walls and cavities in different kinds of PCMS, leading to several resonances and corresponding absorption peaks as may be observed in the results shown in Figures 6 to 7(a) to (d). The truss formation makes the structure highly susceptible to more local resonances, since separate bars or collections of bars can resonate locally, and at resonance the sound wave is damped, leading to higher acoustic absorption. This may also occur at sub-harmonic frequencies of resonances due to medium non-linearity and other factors.

Figure 6 shows that the aluminum pyramidal MicroTruss® PCMS manifests strongly resonant acoustic behavior, and the absorption coefficient exceeds 0.5 in three short frequency bands within the range tested for the 100 mm diameter sample examined in the impedance tube. It should be noted that maximum acoustic performance is generally taken to be an acoustic absorption coefficient of unity at the specific excitation frequencies, but in practice over a wide frequency range including such frequencies, owing to uncertainties. The stainless steel honeycomb MicroTruss® PCMS behaves similarly, but to a lesser extent because its much thinner and more flexible vertical panels formation is less resonant than the pure struts formation of the pyramidal PCMS. The aluminum prismatic triangular channel PCMS is the stiffest and most massive, and has only a few channel compartments. Figure 6 shows its acoustic absorption to be extremely low over the spectrum except for the narrow bands of about 400 Hz-800 Hz, and another at about 4000 Hz where it is a little higher but still low. This reflects the open structure of the material. Air is essentially unconfined in structures with this kind of architecture, and the materials are sonorous and rigidly connected, and thus the structure cannot act as a sound deadener.

The response patterns appear to be quite logical. Assuming perfect fit in the impedance tube, the amount of confined air within the structure, which also contributes to acoustic absorption, is most for the aluminum pyramidal PCMS, less for the stainless steel triangular honeycomb PCMS, and much less for the aluminum prismatic triangular-channel PCMS. The pyramidal aluminum MicroTruss® PCMS seems to perform best in this group, as it has the most air cushion between its skins, and the response shows the typical structural resonance peaks. Its response appears to be more strongly frequency-dependent. The stainless steel triangular honeycomb structure behaves to a lesser extent like the previous sample for similar reasons, except that, as less air is confined mid-structure, and the geometry is less solid than for the aluminum pyramidal MicroTruss®, thus the absorption is less, as is the frequency dependence. The aluminum triangular channel prismatic MicroTruss® PCMS is much more solid than the previous two and has the least enclosed air volume. The absorption is thus much less. This sample is therefore not likely to be deployed for the sake of its acoustic absorption capability.

However, this group of materials being highly multifunctional is very useful and if the results show any deficiency in a particular property, it could be remedied, by augmentation with a compensatory material, or else by appropriate re-design of the necessary section to include features that provide multiple internal reflections of sound, etc. The aluminum prismatic MicroTruss® is a heavy block structure with thicker dimensions of sections inside it than the other PCMS materials. Hence, its absorption is generally low since the structure cannot be easily set into motion by air pressure vibration, and is only slightly more acoustically absorptive at the lower frequencies than at the higher frequencies.

7.3 Vibration Response

Figure 7(a) shows the vibration response spectrum diagram for the aluminum prismaticMicroTruss® PCMS, a display of the most accurate rendering of the vibration frequency response function (FRF) with different useful annotations. The fact of the structure's complexity is obvious, on account of having many resonances. Apart from the fact that distributed systems have an infinite number of resonances, physical complexity facilitates more deformation modes and local resonances in the structure. The resonances are well spaced out and distinct, suggesting that the bending vibration modes are clear and not significantly affected by mixed modes and distortions.

Figure 7(b) shows the vibration response of the aluminum pyramidal MicroTruss® PCMS, while Figures 7(c) shows that of the stainless steel triangular honeycomb PCMS. The stiffer a structure is, the less its deflection under a similar excitation. The fundamental resonance frequency is about twice that of the aluminum pyramidal MicroTruss® PCMS. This shows that the stainless steel honeycomb PCMS is significantly stiffer than the pyramidal MicroTruss® PCMS, but not as stiff as the triangular-channelaluminum prismatic MicroTruss® PCMS. The stainless steel triangular honeycomb PCMS can be therefore expected to perform quite well in limiting vibrations in the automotive or other applications, although the prismatic MicroTruss® PCMS would deflect even less. However, weight considerations have to be weighed as well.

From the mode shapes of Figure 9(b), the plate mode shape patterns of the stainless steel triangular honeycomb PCMSare not evident on either plate skin for the different modes, unlike in the case of the triangular-channel aluminum prismatic PCMS in Figure 9(a), but are generally observed on the vertical plates of the honeycomb core. The reason appears to be that the face skins here are much thinner than those of the aluminum prismatic PCMS, and so are the vertical plate members of the stainless steel honeycomb core. These plates therefore have more freedom to deflect than in the latter PCMS. Moreover, the vertical stiffness of the stainless steel honeycomb core is in this case much higher than the lateral stiffness. This structure therefore essentially constrains the face skins from significant deflections. All these observations comprise useful inputs into how the PCMS constructions should be designed in order to achieve particular, desired vibration responses.

7.4 Sensitivity of Vibration Response to Precise Location of Cut from Stock

It should be mentioned here that these samples had been cut from rectangular block specimens which we got from the Cellular Material Inc. (CMI) company, to fit inside the impedance tube. The criticality of accurately selecting the coordinates of the cut was noticed. Apparently this significantly affects the vibration behavior of the material.A parametric study was done on different cuts of circular samples (100 mm diameter) from the rectangular aluminum and stainless steel PCMS block materials. The cuts were made digitally using the Unigraphics software. The aluminum samples were classified according to the gap (the distance between the lower extremity of the hanging lip and the top of the lower skin) as shown in Figure 8 below. Each cut corresponds to a different location of the center of the 100 mm circle. The variation between all these centers was no more than 2 mm.

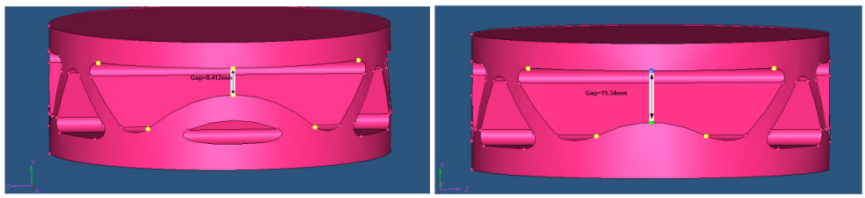

Figure 8. Gaps for two different aluminumprismatic MicroTruss® PCMS samples

7.4.1 Aluminum Triangular Channel Prismatic MicroTruss®

Digital Abaqus Cuts			
Cut #	Mode 1	Mode 2	Mode 3
1	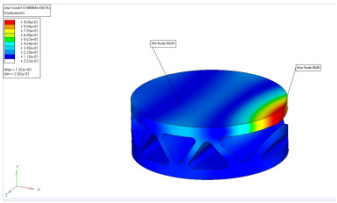 *[f_nExpt (Hz) = 8740]* f_nAbaqus = 8997 Hz max deflection, d_{max}= 1.02 mm	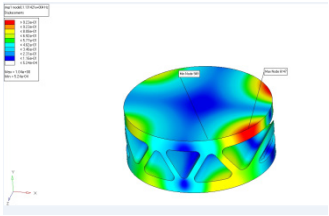 11314 1.04	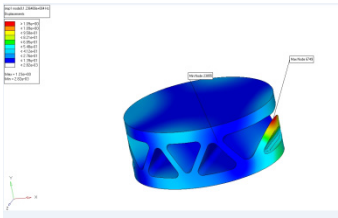 12364 1.23
2	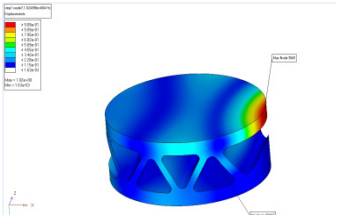 10244 1.02	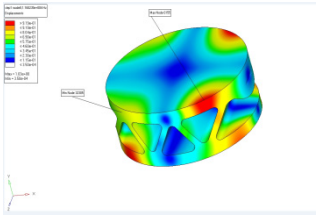 11602 1.03	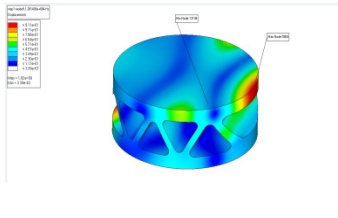 12814 1.02
3	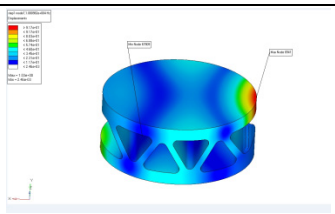 10810 1.03	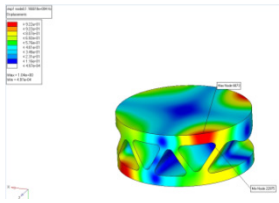 11666 1.04	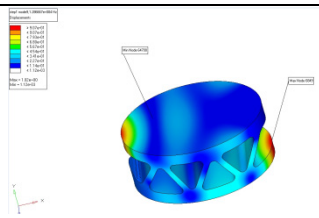 12867 1.02
4	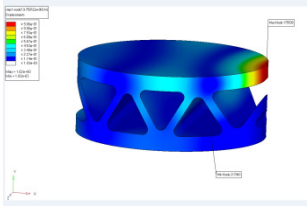 9760 1.02	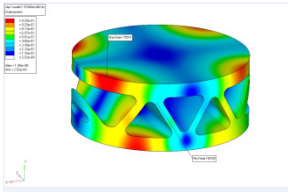 11518 1.05	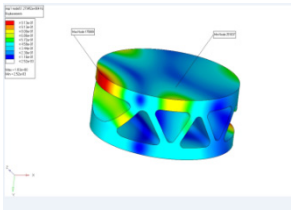 12735 1.03
5	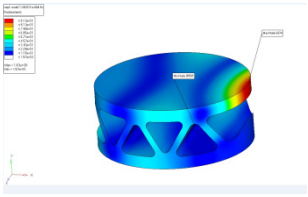 10632 1.03	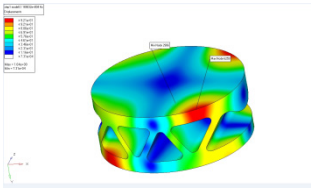 11650 1.04	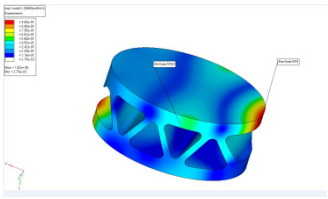 12855 1.02
6	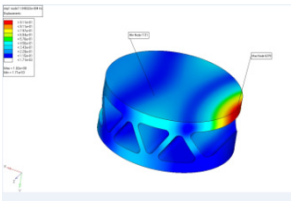 10483 1.02	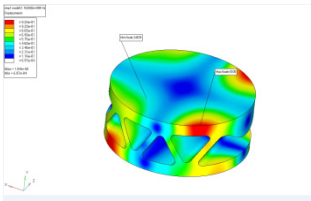 11626 1.04	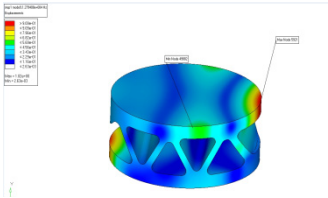 12794 1.02

7	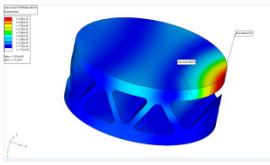 9571 1.02	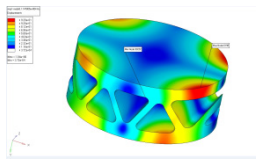 11478 1.04	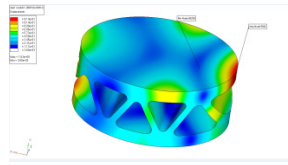 12600 1.03
8	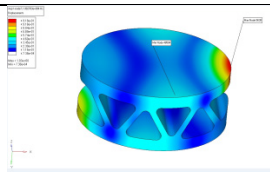 10828 1.03	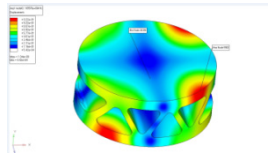 11660 1.04	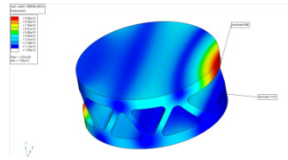 12809 1.02

Figure 9. (a) Sensitivity of vibration response to precise location of cut from stock of aluminum triangular-channel MicroTruss® ™ PCMS – 1st three mode shapes

Figure 9(a) shows the vibration response of the aluminum triangular-channel MicroTruss® PCMS. Its fundamental frequency is more than thrice that of the aluminum pyramidal MicroTruss® PCMS, showing essentially how much stiffer it is. The plate mode shape patterns are evident on either plate skin for the different modes, but these are modified by the two facts that they are connected by the triangular-channel core structure, and also the inevitable asymmetry resulting from cutting a circular portion of specific dimension from a rectangular grid stock material. This case is of great practical importance because in real life, these structures have to be cut into various arbitrary shapes to fit parts being manufactured. The graphical and numerical data presented in Figure 9(a) show clearly that mode shape, resonance frequencies, deflections and stress distributions are sensitive to exactitude of geometry. These geometries are obtained by taking eight different starting centers in a regular rectangular blank of the aluminum triangular-channel PCMS, and digitally cutting the 100 mm circular section. The consequent non-trivial variations in the resulting modal and stress distributions forcefully demonstrate the necessity for accurate and identically-repeatable excision of the desired part from the material stock in order to avoid such variations and departures from intended design values.

7.4.2 Stainless Steel Triangular Honeycomb PCMS

Digital Abaqus cut # 1		
mode	Defln. (f_n Hz, d_{max} mm)	Von Mises stress (MPa)
1	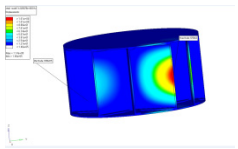 f_nExpt = 4250 4020 1.14	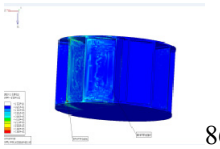 860
2	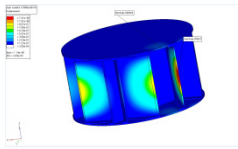 4172 1.14	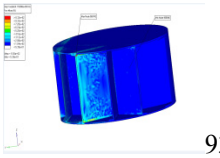 936
3	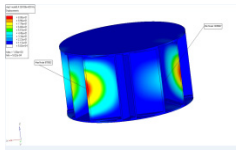 4324 1.00	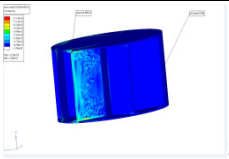 803

Digital Abaqus cut # 2		
mode	Defln. (f_n Hz, d_{max} mm)	Von Mises stress (MPa)
1	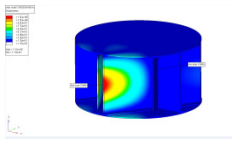 3563 1.16	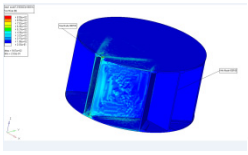 967
2	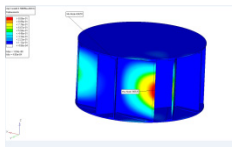 3788 1.00	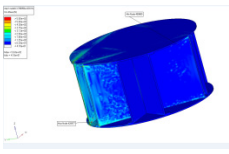 563
3	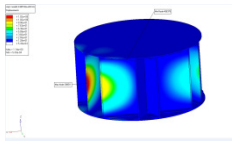 3865.2 1.14	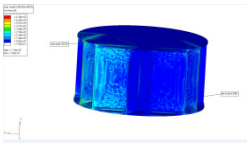 716

Digital Abaqus cut # 3		
mode	Defln. (f_n Hz, d_{max} mm)	Von Mises stress (MPa)
1	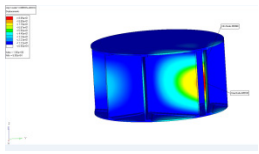 3499.9 1.00	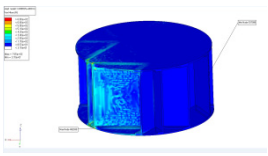 765
2	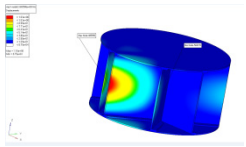 3603.5 1.16	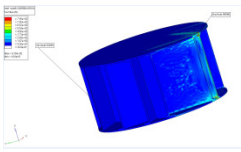 838
3	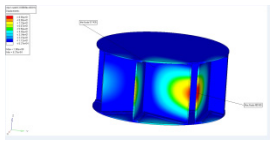 3836.7 1.00	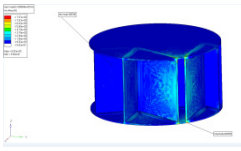 852

Digital Abaqus cut # 4		
mode	Defln.. (f_n Hz, d_{max} mm)	Von Mises stress (MPa)
1	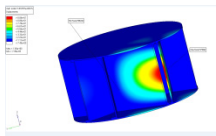 3674.8 1.00	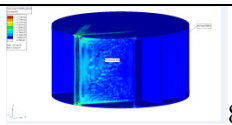 871

2	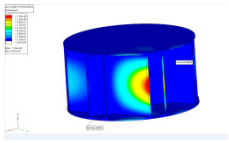 3757.8 1.16	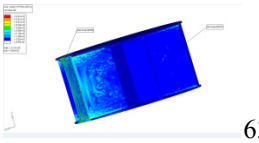 631
3	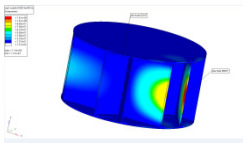 4032 1.14	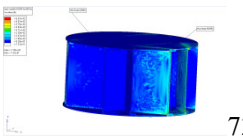 739

Digital Abaqus cut # 5		
mode	Defln.. (f_n Hz, d_{max} mm)	Von Mises stress (MPa)
1	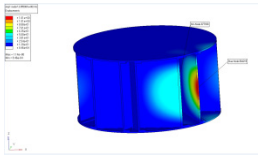 3856 1.14	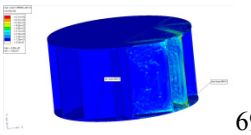 698
2	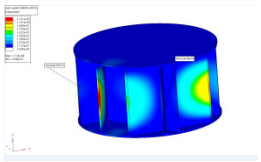 4266.4 1.14	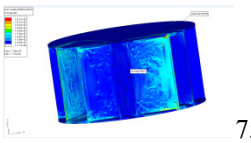 754
3	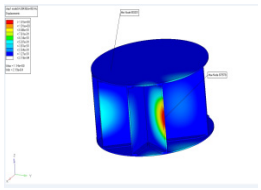 4284.4 1.14	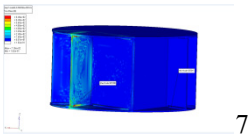 719

Digital Abaqus cut # 6		
mode	Defln.. (f_n Hz, d_{max} mm)	Von Mises stress (MPa)
1	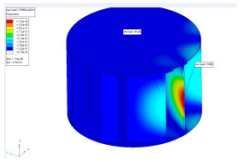 3789 1.16	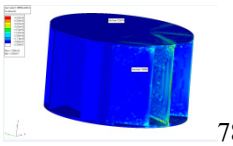 780
2	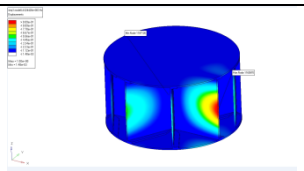 4024 1.00	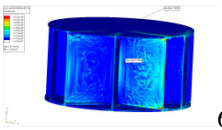 641

3	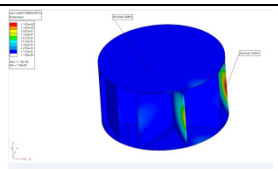 4269.8 1.15	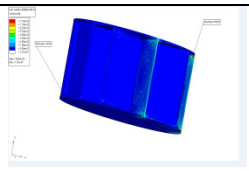 808

Digital Abaqus cut # 7		
mode	Defln.. (f_n Hz, d_{max} mm)	Von Mises stress (MPa)
1	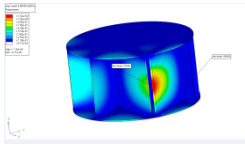 3495.8 1.15	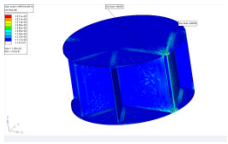 1050
2	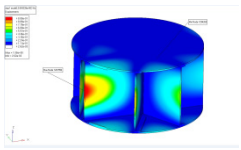 3643 1.00	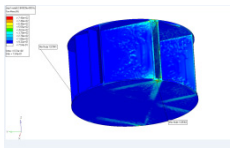 833
3	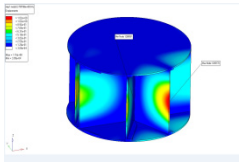 3785.8 1.15	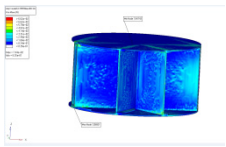 744

Digital Abaqus cut # 8		
mode	Defln.. (f_n Hz, d_{max} mm)	Von Mises stress (MPa)
1	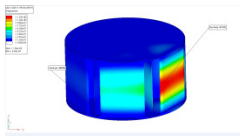 3118 1.16	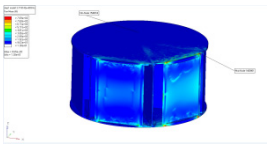 865
2	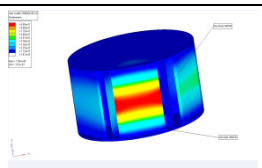 3268.4 1.00	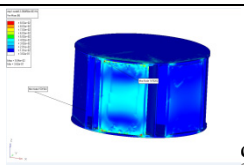 904
3	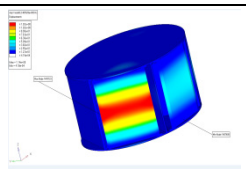 3487.6 1.14	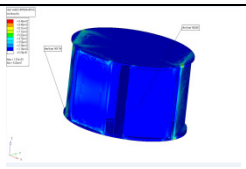 1070

Figure 9. (b) Sensitivity of vibration response to precise location of cut from stock of stainless steel triangular honeycomb PCMS-fundamental frequency, max. deflection and Von Mises stress

The effects of the inevitable asymmetry resulting from cutting a circular portion of specific dimension from a rectangular grid stock material are probed in this case as well. The graphical and numerical data presented in Figure 9(b) show clearly that mode shape, resonance frequencies, deflections and stress distributions are sensitive to exactitude of geometry. This probe is accomplished by taking eight different starting centers in a regular rectangular blank of this PCS, and digitally cutting out the 100 mm circular section. The resulting variations in the modal and stress distributions once more strongly demonstrate the requirement for accurate and identically-repeatable removal of the desired part from the material stock in order to avoid such variations and unintended departures from design values.

8. Conclusion

Three novel metal PCMS types have been studied for their vibration and acoustic performances. These were the aluminum pyramidal MicroTruss® PCMS, the stainless steel triangular honeycomb PCMS, and the aluminum (triangular-channel) prismatic MicroTruss® block PCMS. The PCMS materials were tested in this work for acoustic response using the impedance tube setup, and the vibration behavior using the PULSE system. To verify the experimental results, finite element simulation was used to get the natural frequencies, and mode shapes, for each of the samples.

From this work, it could be concluded that, as presently designed, the PCMS materials could offer some degree of vibration amelioration, but little acoustic containment. However, there seems to be a wide possibility of re-design and material augmentation that will effectively address these points, in significantly improving both acoustic and vibration performances. Besides, PCMS have great potential for utilization as metamaterials to more precisely control sound and vibration.

References

Andrea, Zent. A., & Long, J. T. (2007). *Automotive Sound Absorbing Material Survey Results*. 2007 SAE International, Paper # 2007-01-2186.

Ayorinde, E. O., Al-Zubi, M., Dundar, A., & Witus, G. (2012). Experimental and numerical analysis of membrane-patterned meta-materials paper IMECE2012-88752. *ASME International Mechanical Engineering Congress & Exposition*, November 9-15, 2012, Houston, Texas, USA.

Birman, V., (2005). Shape memory elastic foundation and supportsfor passive vibration control of composite plates. *International Journal of Solids and Structures, 45*, 320-335.

Chevillotte, F., Perrot, C., & Pennelton, R. (2010). Microstructure based model for sound absorption predictions of perforated closed-cell metallic foams. *Journal of the Acoustic Society of America, 128*(4), 1766-1776. http://dx.doi.org/10.1121/1.3473696

de Bedout, J. M., Franchek, M. A., Bernhard, R. J., & Mongeau, L. (1997). Adaptive-passive noise control with self-tuning helmholtz resonators. *Journal of Sound and Vibration, 202*(1), 24, 109-123. http://dx.doi.org/10.1006/jsvi.1996.0796

Fang, Q., Li, Y., & Fu, X. (2012). Studies on vibration control of beam by damping material. *IEEE International Conference on Computer Distributed Control and Intelligent Environmental Manufacturing*, 5-6 March 2012, IEEE Paper 978-0-7695-4639-1/12, 647-650.

Hong, Z., Bo, L., Guangsu, H., & Jia, H. (2007). A novel composite sound absorber with recycled rubber particles. *Journal of Sound and Vibration, 304* (1-2), 400-406. http://dx.doi.org/10.1016/j.jsv.2007.02.024

Huang, G. L., & Sun, C. T. (2010). Band gaps in a multi-resonator acoustic metamaterial, Transactions of the ASME. *Journal of Vibration and Acoustics, 132*(3), 031003, 1-6.

Islam, M. T., & Newaz, G. (2012). Metamaterials with mass-stem array in acoustic cavity. *Applied Physics Letters, 100*, 011904, 1-4.

Kargarnovin, M. H., Najafizadeh, M. M., & Viliani, N. S. (2007). Vibration control of a functionally graded material plate patched with piezoelectricactuators and sensors under a constant electric charge. *Journal of Smart Materials and Structures, 16*, 1252-59. http://dx.doi.org/10.1088/0964-1726/16/4/037

Mohammad, Al-Zubi. (2012). *Investigation and improvement of noise, vibration and harshness (NVH) properties of automotive panels.* (January 1, 2012). ETD Collection for Wayne State University. Paper AAI3527806. http://digitalcommons.wayne.edu/dissertations/AAI3527806

Pfretzschner, J., & Rodriguez, R. (1999). Acoustic properties of rubber crumbs. *Polymer Testing, 18*(2), 81-92. http://dx.doi.org/10.1016/S0142-9418(98)00009-9

Queheillalt, D. T., Douglas, T., Yellapu Murty, & Wadley, H. N. G. (2008). Mechanical properties of an extruded pyramidal lattice truss sandwich structure. *Scripta Materialia, 58*, 76-79. http://dx.doi.org/10.1016/j.scriptamat.2007.08.041

Sypeck, D. J., & Wadley, H. N. G. (2002). Cellular meta truss core sandwich structures. *Advanced Engineering Materials, International Journal of Solids and Structures, Special Issue, 4*(10), 759-764.

Tian, J., Kim. T., Lu, T. J., Hodson, H. P., Queheillalt, D. T., & Wadley, H. N. G. (2004). The effects of topology upon fluid-flow and heat-transfer within cellular copper structures. *International Journal of Het and Mass Transfer, 47*(14-15), 3171-3186. http://dx.doi.org/10.1016/j.ijheatmasstransfer.2004.02.010

Wadley, H. N. G., Fleck, N. A., & Evans, A. G. (2003). Fabrication and structural performance of periodic cellular metal sandwich structures. *Composites Science and Technology, 63*, 2331-2343.

Wadley, H. N. G. (2002). Cellular metals manufacturing, Advanced Engineering Materials. *International Journal of Solids and Structures, Special Issue, 4*(10), 726-733.

Wei, Z., Deshpande, V. S., Evans, A. G., Dharmasena, K. P., Queheillalt, D. T., Wadley, H. N. G., … Kiddy, K. (2008). The resistance of metallic plates to localized impulse. *Journal of the Mechanics and Fluids of Solids, 56*, 2074-2091. http://dx.doi.org/10.1016/j.jmps.2007.10.010

Xu, Z., Huang, Q., Zhao, Z., & Zhang, Q. (2009). Noise and vibration control of composite material plate based on frequency shift using topology optimization, (2009). *IEEE Joint Conference of the 2009 Symposium on Piezoelectricity, Acoustic Waves, and Device Applications (SPAWDA) and 2009 China Symposium on Frequency Control Technology*, 17-20 Dec. 2009, IEEE Paper 978-1-4244-4949-1/09, 217-220.

Yang, B. (2005). *Stress, strain, and structural dynamics: An interactive handbook of formulas, solutions, and MATLAB toolboxes*. Elsevier Academic Press.

Yu, G., & Cheng, L. (2009). Location optimization of a long T-shaped acoustic resonator array in noise control of enclosures. *Journal of Sound and Vibration, 328*(1–2), 42-56.

Copyrights

Copyright for this article is retained by the author(s), with first publication rights granted to the journal.

This is an open-access article distributed under the terms and conditions of the Creative Commons Attribution license (http://creativecommons.org/licenses/by/3.0/).